Cerebral Cortex, 2019;00: 1–18

doi: 10.1093/cercor/bhz281
Advance Access Publication Date:
Original Article

ORIGINAL ARTICLE

Differential Effects of Open- and Closed-Loop Intracortical Microstimulation on Firing Patterns of Neurons in Distant Cortical Areas

Alberto Averna[1,2,3], Valentina Pasquale[3], Maxwell D. Murphy[4], Maria Piera Rogantin[6], Gustaf M. Van Acker[7], Randolph J. Nudo[4,5], Michela Chiappalone[1] and David J. Guggenmos[4,5]

[1]Rehab Technologies, Istituto Italiano di Tecnologia, 16163 Genova, Italy, [2]Department of Neuroscience, Rehabilitation, Ophthalmology, Genetics and Maternal and Child science (DINOGMI), University of Genova, 16145 Genova, Italy, [3]Neuroscience and Brain Technologies, Istituto Italiano di Tecnologia, 16163 Genova, Italy, [4]Department of Physical Medicine and Rehabilitation, University of Kansas Medical Center, Kansas City, KS 66160, USA, [5]Landon Center on Aging, University of Kansas Medical Center, Kansas City, KS 66160, USA, [6]Department of Mathematics, University of Genova, 16146 Genova, Italy and [7]Department of Molecular and Integrative Physiology, University of Kansas Medical Center, Kansas City, KS 66160, USA

Address correspondence to Michela Chiappalone, Department of Neuroscience and Brain Technologies (NBT) and Rehab Technologies, Istituto Italiano di Tecnologia (IIT), Via Morego 30, 16163 Genova, Italy. Email: michela.chiappalone@iit.it.

Michela Chiappalone and David Guggenmos contributed equally to this work.

Abstract

Intracortical microstimulation can be used successfully to modulate neuronal activity. Activity-dependent stimulation (ADS), in which action potentials recorded extracellularly from a single neuron are used to trigger stimulation at another cortical location (closed-loop), is an effective treatment for behavioral recovery after brain lesion, but the related neurophysiological changes are still not clear. Here, we investigated the ability of ADS and random stimulation (RS) to alter firing patterns of distant cortical locations. We recorded 591 neuronal units from 23 Long-Evan healthy anesthetized rats. Stimulation was delivered to either forelimb or barrel field somatosensory cortex, using either RS or ADS triggered from spikes recorded in the rostral forelimb area (RFA). Both RS and ADS stimulation protocols rapidly altered spike firing within RFA compared with no stimulation. We observed increase in firing rates and change of spike patterns. ADS was more effective than RS in increasing evoked spikes during the stimulation periods, by producing a reliable, progressive increase in stimulus-related activity over time and an increased coupling of the trigger channel with the network. These results are critical for understanding the efficacy of closed-loop electrical microstimulation protocols in altering activity patterns in interconnected brain networks, thus modulating cortical state and functional connectivity.

Key words: anesthesia, electrical stimulation, forelimb, motor cortex, neuronal plasticity, neurons, neurophysiology, rats, somatosensory cortex

Introduction

Focal, invasive electrical stimulation techniques, such as intracortical microstimulation (ICMS) and deep brain stimulation (DBS), have the ability to target and directly depolarize a relatively small population of neurons compared with noninvasive techniques such as transcranial magnetic stimulation or transcranial direct current stimulation. While ICMS is typically employed in invasive animal studies, focal properties of invasive electrical stimulation have made DBS advantageous for implementation into clinical tools for treating a variety of neurological conditions, such as epileptic seizures (Fisher et al. 2010; Kerrigan et al. 2004; Lee et al. 2006; Morrell 2011) and Parkinson's disease (Anderson et al. 2005; Bronstein et al. 2011; Deuschl et al. 2006; Little et al. 2013; Weaver et al. 2012). ICMS, specifically, is also being investigated for the direct treatment of conditions such as pain and depression, among others, and in brain–computer interfaces to augment or restore lost function after injury, such as for visual (Bradley et al. 2005; Davis et al. 2012; Dobelle and Mladejovsky 1974; Schmidt et al. 1996; Torab et al. 2011) or somatosensory (Berg et al. 2013; Tabot et al. 2013; Thomson et al. 2013) neuroprosthetic devices. While the local physical and neurophysiological effects of this type of stimulation have been described in detail (Cohen and Newsome 2004; Histed et al. 2013; Ranck Jr 1975; Tehovnik et al. 2006; Tehovnik and Slocum 2013), there is much less information on how focal stimulation impacts areas distant from the immediate spread of the electrical current or across multisynaptic pathways. This is an important consideration, as these stimulated regions are not isolated (Fox et al. 2014) but have anatomical connections with several other regions within the brain. The effectiveness of treatments that relies on focal electrical stimulation is likely dependent on the modulation of these pathways, but there are still open questions about how this stimulation affects the firing patterns within these distant regions.

The impact of focal electrical stimulation on distant brain regions may be even more pertinent in "closed-loop" designs, in which intrinsic neural activity drives stimulation protocols. One such design, named activity-dependent stimulation (ADS), uses the occurrence of action potentials (spikes) in one neuron to trigger stimulation at another location or electrode site. ADS relies on the concept of Hebbian plasticity, in which repeated concomitant firing of two neurons will strengthen the connection between them. In closed-loop systems, secondary neuronal firing is induced via the stimulation. By artificially pairing spike-firing in one population of neurons with focal electrical stimulation of a second population of neurons, it may be possible to shape the efficacy of specific neural pathways in vivo (Guggenmos et al. 2013; Jackson et al. 2006; Nishimura et al. 2013a; Rebesco and Miller 2011; Rebesco et al. 2010).

The purpose of the present study was to determine if neural firing patterns in distant regions are altered in response to short-duration stimulation sessions in anesthetized rats. To model a relevant system in vivo, the rostral forelimb area (RFA), a premotor area, was used for neural recordings, while either closed-loop ADS or random stimulation (RS) was delivered to somatosensory cortex (S1), either in the S1 forelimb area (S1FL) or in the S1 barrel field (S1BF). These areas share reciprocal neuroanatomical connections, providing an anatomical framework for changing synaptic efficacy (Mohammed and Jain 2016). In a previous study, we found that an ADS protocol in a chronic injury model, i.e., pairing the occurrence of spikes in RFA with ICMS applied to S1, led to increased evoked firing within RFA over a period of several days (Guggenmos et al. 2013). In the present study, we investigated ADS effects under the more controlled conditions of an anesthetized preparation, enabling us to assess alterations in RFA spike firing patterns over single stimulation sessions. This preparation allowed us to more readily test various parameters such as stimulation condition (ADS or RS) and stimulation location (S1FL or S1BF). Because these regions are functionally and anatomically connected, the results may be generalizable to other, similarly interconnected regions. Understanding changes in neuronal activity in distant areas in response to focal closed-loop and random ICMS may lead to more effective brain stimulation protocols that target functional connectivity within specific brain pathways, and thus, to improve current therapeutic devices for neurological disorders.

Material and Methods

Animals

All experiments were approved by the University of Kansas Medical Center Institutional Animal Care and Use Committee. A total of 23 adult, male Long-Evans rats (weight: 350–400 g, age: 4–5 months; Charles River Laboratories, Wilmington, MA, USA) were used in this study.

Surgical Procedures

Prior to surgery, anesthesia was induced with gaseous isoflurane within a sealed vaporizer chamber followed by bolus injections of ketamine (80–100 mg/kg IP) and xylazine (5–10 mg/kg). Throughout the procedure, pinch and ocular reflexes were assessed every 15 min. Anesthesia was maintained throughout the procedure with bolus injections of ketamine (10–100 mg/kg/hr IP or IM) given whenever there was a positive reflex response.

A midline incision was made to expose the skull. A laminectomy was performed at the cisterna magna to drain cerebrospinal fluid, thus controlling brain edema. A craniectomy was made over the extent of premotor cortex (PM or RFA), primary motor cortex (M1 or Caudal FL—CFA), and primary somatosensory cortex (S1) using a drill with a burr bit. Saline was applied periodically to avoid heat generation by the drill. The dura was resected over the extent of the opening. Silicone oil (dimethylpolysiloxane) was applied to the cortical surface to avoid desiccation and facilitate electrophysiological procedures. Following the experiment, rats were humanely euthanized using pentobarbital (390 mg IP).

Identification of Cortical Areas of Interest

Upon completion of the surgical procedure, a picture of the vascular pattern of the cortical surface was taken and uploaded to a graphics program (Canvas GFX, Inc.), where a 250-μm virtual grid was overlaid onto the image. The location of RFA was determined using standard ICMS protocols (Kleim et al. 2003). Briefly, a glass microelectrode (10–25 μm diameter) filled with saline was systematically inserted into the cortex at sequential grid intersections using the vascular pattern as a visual reference a

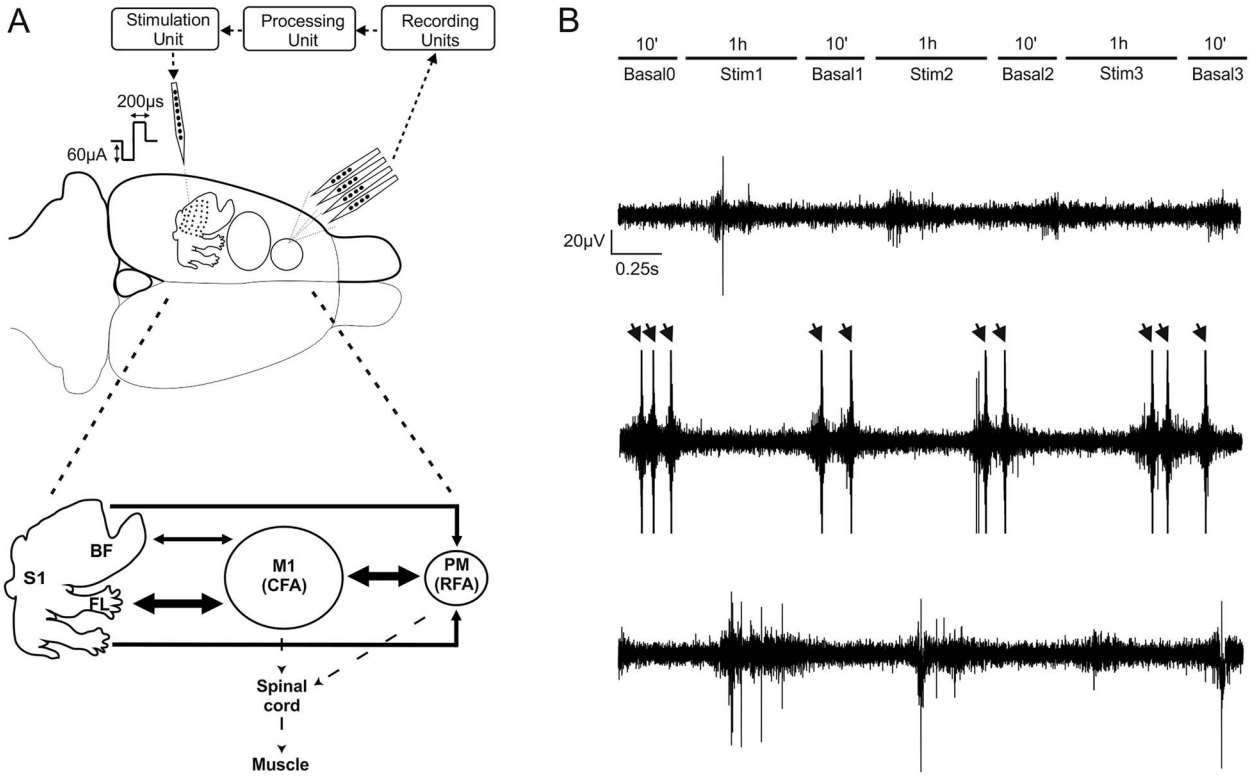

Figure 1. Recording and stimulation experimental paradigm. (*A*) Extracellular recordings were obtained through a four-shank, 16-contact microelectrode probe in anesthetized rats. Signals were acquired ("Recording Unit") and processed to detect single-unit activity ("Processing Unit") selected by the user and employed as reference neuron to trigger a stimulus pulse to a channel on the single-shank microelectrode ("Stimulation Unit"). A summary diagram showing the main cortico-cortical anatomical connections between regions is shown in Fig. 1A, bottom. Arrow thickness corresponds to the amount of labeling (medium or high) suggested by Zakiewicz (Zakiewicz et al. 2014). (*B*) Recording sessions (in RFA) consisted of three 1-hour intermittent periods of stimulation with either ADS or RS to either S1BF or S1FL, each separated by 10-min periods of no stimulation. Example traces in a representative experiment of extracellular recording during the first basal period (Basal0, Top), during the first stimulation session (Stim1, Mid), and during the second basal period, after the stimulation (Basal1, Bottom). Arrows represent the electrical stimulation artifacts.

depth of ~1700 µm (impedance at 1000 Hz = ~500 kΩ). Stimulus trains of 13–200 µs pulses at 333 Hz were applied at 1-Hz intervals using a stimulus isolator (BAK Electronics). Current was increased until a visible movement about a joint was observed, up to a maximum current of 80 µA. RFA was defined as the region in the rostral portion of frontal cortex where ICMS evoked forelimb movements. RFA was bordered caudally by a region where ICMS evoked neck and trunk movements, and medially by face and jaw movements (Kleim et al. 1998). RFA was easily distinguished from CFA based on its relatively smaller size and more rostral and circumscribed location.

Somatosensory areas were identified by correlating neural responses evoked by slight indentation of the skin or vibrissae brushing. A single-shank, 16-channel Michigan style electrode (A1x16-5 mm-100-703-A16, NeuroNexus) was lowered to a maximum depth of ~1700 µm and attached to a unity gain headstage connected to a digitizing pre-amplifier and piped to a processing unit (Tucker-Davis Technologies—TDS). Activity of all 16 channels was displayed in real time on a computer screen for visual discrimination of spikes, and a user selected channel was sent to a speaker for auditory discrimination of spikes. S1FL was defined as the region where a consistent, short-latency spike discharge was evoked in response to light stimulation of a small receptive field on the wrist, paw, or digits. S1BF was defined by a constant short-latency spike discharge evoked by deflection a single or small number of the mystacial vibrissae. For each sensory area, multiple cortical sites were characterized to ensure the reliability of the S1 target location.

Experimental Protocol

Following the identification of RFA and S1 FL/BF, a four-shank, 16-contact site microelectrode probe (A4x4-5 mm-100-125-177-A16, NeuroNexus) was placed within RFA at a depth of ~1600 µm for recording purposes (Fig. 1A). An active unity gain connector was attached to the probe and connected through a pre-amplifier for recording (TDT). Passband filtered data (300–5000 Hz) underwent online spike detection using an embedded principal component sorting algorithm (PCSort) through which neural data could be identified and separated from noncellular data in near real-time. An activated single-shank, 16-contact microelectrode probe with an impedance of 100–300 kΩ measured at 1 KHz (A1x16-5 mm-100-703-A16, NeuroNexus) was inserted into the somatosensory area to a depth of ~1500 µm for stimulation purposes (Fig. 1A). Rats were randomly assigned to one of four experimental groups based on stimulation condition (ADS or RS) and stimulation location (S1FL or S1BF). Thus, each rat was subjected to only one set of experimental parameters. An additional control group (CTRL)

Table 1 The total number of animals and the number of units examined per experimental condition

Location of the stim electrode	Stimulation type			Total
	RS	ADS	CTRL	
S1 BF	4/113	6/180	—	10/293
S1 FL	4/103	5/114	4/81	13/298
Total	8/216	11/294	4/81	23/591

received no stimulation (cf. Table 1 for group assignments). For all groups, the experimental protocol consisted of four 10-min periods, where the stimulator was set to deliver 0 µA (i.e., Basal0, Basal1, Basal2, and Basal3), interspersed with three 1-h periods where stimulation was delivered at 60 µA (Stim1, Stim 2, and Stim3), for a total of ~3 h and 40 min of recorded data for a single experimental session (Fig. 1B).

In four rats (1 ADSBF, 2 ADSFL, and 1 RSBF) from the total of 23, recording sessions were truncated after the first 2-h-long stimulation periods (after Basal2), due to a substantial decrease in neural activity, either due to the loss of the trigger neuron, or technical issues related to environmental noise, and/or anesthetic complications. However, data from these rats up to the time that the protocol was terminated were considered to be valid and have been included in the analyses. Control experiments underwent the same protocol as ADS, but the stimulator was set at 0 µA for the entire recording session.

Stimulation Paradigms

For all experimental conditions, a single 60-µA balanced biphasic, cathodal-leading stimulation pulse (200-µs positive, 200-µs negative) was delivered into S1 through a single contact site on the electrode (site six, corresponding to the tip of the electrode) on each stimulation trigger. The timing and pulse shape parameters are nearly identical to those used in previous studies to induce behavioral changes following long-term, chronic ADS (Guggenmos et al. 2013; Jackson et al. 2006). Stimulation currents were limited to 60 µA (12 nC/phase and a charge density of 1.7 mC/cm2) primarily due to the finding that this intensity has a negligible effect on the electrode-tissue interface (Chen et al. 2014) and on the neuronal tissue itself (Rajan et al. 2015). Stimulation pulses were delivered using a stimulus isolator and a passive headstage (MS16 Stimulus Isolator, TDT). A custom script written for the TDT DSP allowed for stimulation triggering in one of two conditions. For RS, an internal random number generator combined with a set of gates would trigger stimulation with a Poisson distribution with a mean stimulation rate of 7 Hz. For ADS, a user-defined spike profile was identified from the PCSort component based on the visual assessment of amplitude, signal-to-noise ratio, and rate. In ADS, there was an imposed 10-ms delay (2.5-ms hardware delay, 7.5-ms user-defined software delay) between spike detection and stimulation. For both ADS and RS, there was an imposed 18-ms "blanking" period starting at the initiation of the delivered pulse where the treatment was blocked to prevent any direct stimulation feedback loop.

Data Processing

Data from all 16 channels recorded from the RFA electrode were processed offline for further analysis. Recorded, bandpass-filtered neural data (~300 Hz–3 kHz) was recorded (TDT) at 24.414 kHz per channel and processed using custom MATLAB (The Mathworks) scripts. The Precise Timing Spike Detection, a custom offline spike detection algorithm, was used to automatically perform spike discrimination (Maccione et al. 2009), followed by superparamagnetic clustering (Blatt et al. 1996; Quiroga et al. 2004) to sort the detected spikes, and then a subsequent visual assessment of sorted clusters was used to identify all spikes used in the analysis.

Mean Firing Rate

The neuronal firing rates were evaluated before and after the stimulation by calculating the mean firing rate (MFR) in each period. Neurons whose firing rate was less than 0.01 spikes/s were discarded. Determination of whether the difference in firing rates between two time-points for a given unit significantly deviated from a null (zero centered) distribution was calculated using a bootstrapping method (Slomowitz et al. 2015). The two time-segments to be compared (Basal_i, Basal_{i+1}; $i = 1{:}3$) were divided into 1-min bins and then randomly shuffled 10 000 times into two groups. The differences between the means of the two randomly shuffled groups produced a null-distribution. The real difference was significant if it fell outside of the 95% confidence interval of the null-distribution.

Local Variation Compensate for Refractoriness

The temporal patterns of spike activity exhibited in RFA were evaluated using a revised version of Lv parameter, namely local variation compensate for refractoriness (LvR), as proposed in Shinomoto et al. 2009. LvR measures the local variation of the ISI and describes the intrinsic firing irregularity of individual neurons, without being confounded by firing rate fluctuations (Shinomoto et al. 2009). This metric assumes that rate dependence is caused by the refractory period of a spike, R, which is subtracted from the interspike interval (ISI). The refractoriness constant, R, was optimized to maximize the characterization of firing dynamics of individual neurons in terms of F values, and thus it was set to 5 ms (Shinomoto et al. 2009). The revised local variation LvR equation after several simplifications (Shinomoto et al. 2009) is defined as:

$$\mathrm{LvR} = \frac{3}{n-1}\sum_{i=1}^{n-1}\left(1 - \frac{4I_iI_{i+1}}{(I_i + I_{i+1})^2}\right)\left(1 + \frac{4R}{I_i + I_{i+1}}\right),$$

Where I_i and I_{i+1} are the ith and $i+1$st ISI and n is the number of ISIs. This metric produces a value, ranging from 0 to more than 2, and can be used to classify the individual neuron's activity into "Regular" (approx. 0.5 ± 0.25), "Random" (approx. 1 ± 0.25), and "Bursty" (approx. 1.5 ± 0.25) firing patterns (Shinomoto et al. 2009).

Poststimulus Time Histogram

Poststimulus time histograms (PSTH) (Rieke 1999; Rieke et al. 1997) (1-ms bins, normalized over the total number of stimulation pulses) of stimulus-associated action potentials of each sorted unit were calculated during the 28-ms following stimulus pulses delivered from either S1FL or S1BF. The area under the normalized PSTH curve was used to quantify the total amount of stimulation-evoked neural activity during each stimulation phase.

Population Coupling

Population coupling (PC) is a measure that characterizes the relationship of each neuron to the activity of a larger population (population rate—PR), calculated as the summed activity of all neurons recorded in an area at any moment in time (Renart et al. 2010; Tkačik et al. 2014). This metric estimates the overall synaptic connectivity of each neuron with the cortical network and allows a description of each unit as a chorister (i.e., a neuron generally firing together with the population) or a soloist (i.e., a neuron not synchronized with the population) (Okun et al. 2015). The two categories were defined by selecting the top five scoring neurons as choristers and the lowest five scoring neurons as soloists.

Briefly, the PR was computed by accumulating all the detected spikes with a 1-ms resolution; then, for all the 16 recording channels of RFA, we evaluated the single channel spike train relationship with the PR. The PR has been smoothed with a Gaussian (half width 12 ms) filter and the spikes of the channel used for the computation were not included. Subsequently, we counted the amount of values under the PR curve between 500-ms windows close to the single time stamp of the channel. This total amount was normalized by dividing for the number of the spikes of the channel. The resulting curve (spike-triggered PR—stPR) shows a peak centered at zero (i.e., the PC); its height can be large for some neurons and small or even reversed based on the strength of their relationship with the population activity (i.e., choristers and soloists). To compare PCs across recordings, we implemented the shuffling procedure proposed by Okun et al., and normalized each PC over the median size of the shuffled stPR in each recording (Okun et al. 2015).

We used the PC metrics to investigate the properties of the triggering channel with respect to the activity of the neuronal population under recording. Because the online sorting algorithm used to extrapolate the trigger channel's activity was different from the one used for their offline analysis, the triggered stimulation train and the corresponding single unit trigger identified by our analysis did not necessarily completely match. For this reason, we considered as "trigger channel" activity the spikes detected offline at on the contact site channel chosen for triggering the stimulation, and we run the PC analysis on the offline detected spiking activity without sorting (multiunit activity).

Statistical Model

This study was designed to assess the effect and interactions of stimulation type and area over time on neuronal activity. Because the independence of individual neuron firing rates cannot be assumed within a particular rat and because the distribution of firing rates tends to have a Poisson rather than Gaussian distribution, it is most appropriate to utilize a generalized linear mixed model (GLMM) for repeated measures to fully capture any differences in area and stimulation condition over time rather than a more common analysis such as an ANOVA. We performed all analyses using SAS/STAT® software (Version 9.2 of the SAS System for Windows, SAS Institute Inc.). GLMM is a powerful statistical tool that permits modeling of not only the means of the data (as in the standard linear model) but also their variances as well as within-subject covariances (i.e., the model allows subjects with missing outcomes—unbalanced data—to be included in the analysis).

Within this model, each recorded neuron was treated as a subject (neuron). The model included the two fixed between-subject factors being analyzed: the stimulation condition (with three levels for factor StimCond: RS, ADS, and CRTL) and the stimulation location or "Area" (with two levels for factor Area: S1FL and S1BF). The outcome was a variable measured at the four fixed basal time periods (within-subject factor "Time"). The model also included second- and third-order interactions among the factors (StimCond*Area, StimCond*Time, Area*Time, and StimCond*Area*Time).

Each rat was considered a random factor and implied a different intercept for each rat. The variance-covariance matrix for errors was considered unstructured, as it was different for each subject. The MIXED procedure of SAS, by default, fits the structure of the covariance matrix by using the method of restricted maximum likelihood (Harville 1977), also known as residual maximum likelihood. Finally, the fixed part of the expected values of the basal period recorded at the time t, with the stimulus s applied to the area a, was: $\mu + \tau_t + \alpha_a + \sigma_s + \delta_{t,a} + \gamma_{t,s} + \varepsilon_{a,s} + \gamma_{t,a,s}$, where the parameters τ_t, with $t \in \{1, 2, 3, 4\}$,referred to factor "Time," the parameters α_a, with $a \in \{\text{FL}, \text{BF}\}$, referred to factor "Area," the parameters σ_s, with $s \in \{\text{ADS}, \text{RS}, \text{CTRL}\}$, referred to factor "StimCond," and the parameter $\delta_{t,a}$, $\gamma_{t,s}$, $\varepsilon_{a,s}$, and $\gamma_{t,a,s}$referred to second- and third-order interactions. The reference level of the factor "StimCond" was set to be CTRL first, then to be RS, in order to easily compare the three levels. P values < 0.05 were considered significant.

Results

We investigated the capability of two ICMS stimulation conditions to affect spike rate and temporal patterns of firing in a distant but interconnected cortical regions. In healthy, ketamine-anesthetized rats, multisite microelectrode probes were used to determine the effects of ICMS delivered to somatosensory cortical areas (FL and BF) on spontaneous spike firing rates, regularity of firing patterns, and stimulus-evoked spike firing in RFA.

ICMS Results in Increased Firing Rate in a Distant Cortical Area

First, MFR was compared between the initial basal period (Basal0) and subsequent basal periods (Basal1, Basal2, and Basal3) following each 1-h period of RS or ADS ICMS. Figure 2A illustrates spike firing rates in a representative animal (ICMS in BF, ADS condition) demonstrating an overall increase of firing from Basal0 (top, left) to Basal3 (top, right). The increase in MFR occurred in each of the experimental conditions (ADSBF, ADSFL, RSBF, and RSFL) but not in control experiments (CTRL) (Fig. 2B).

Table 2 contains the global results of hypothesis tests for the considered fixed effects. Main effects and third-order interactions of the effects are described in Table 3.

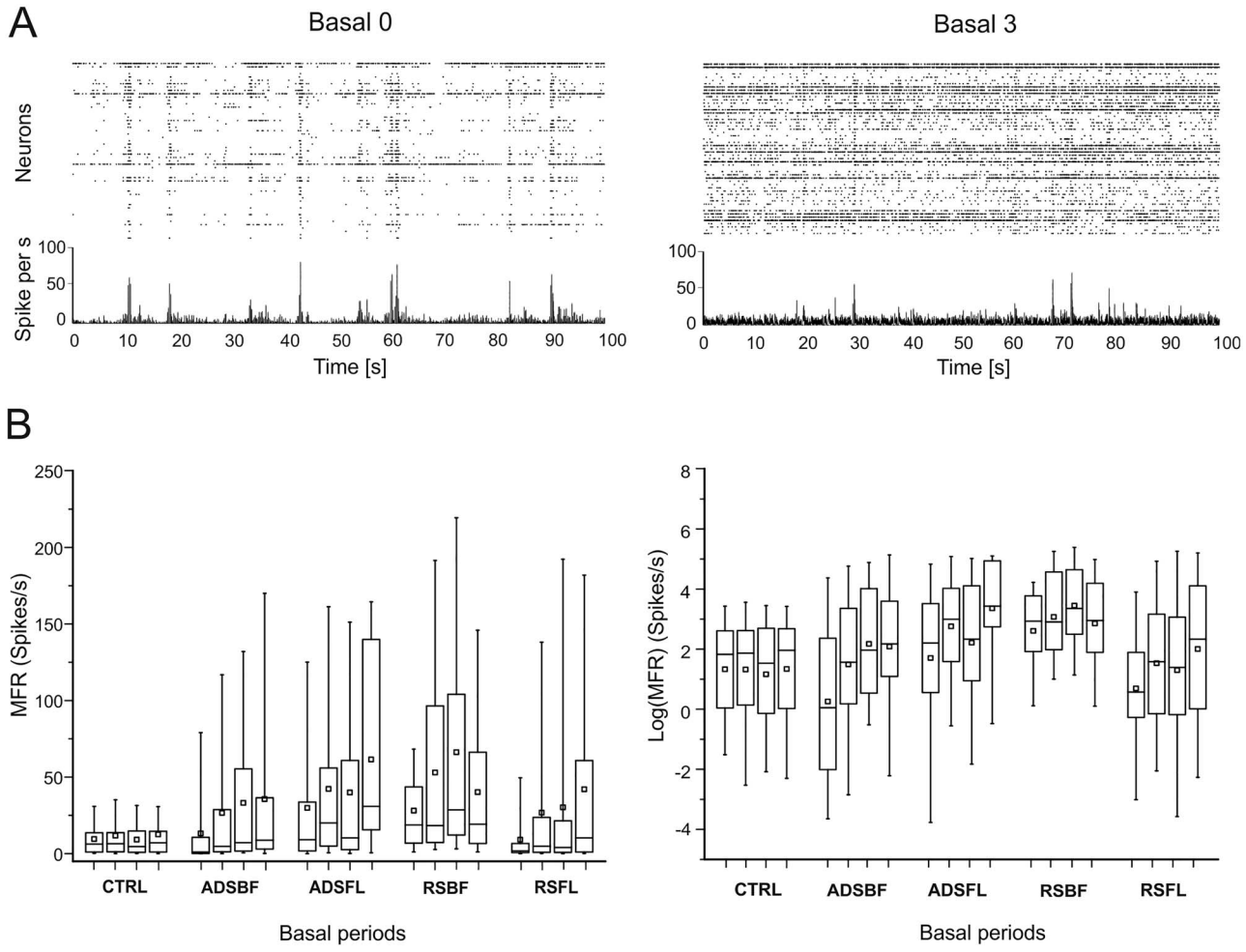

Figure 2. Firing rate analysis. (*A*) Spike rasters (dotted graphs, one row per sorted unit) and corresponding array-wide firing rate (line graphs) measured by summing all spikes detected on the entire array in 1-ms windows during 100-ms time frame of Basal0 (left) and Basal3 (right) for a single representative animal which underwent the ADS protocol in BF. (*B*) Left: Quantitative representation of the MFR distributions for each experimental group (CTRL; ADSBF; ADSFL; RSBF; RSFL) in each Basal phase (0–3). Right: Representations of the Log (MFR) distributions of each experimental group and for each basal period. Data are summarized in box plots, where the horizontal lines denote the 25th, median, and 75th percentile values and the whiskers denote the 5th and 95th percentile values; the square inside the box indicates the mean of each data set. Statistical analysis is reported in Tables 2 and 3.

Table 2 Results of general linear mixed effects model on the logarithmic firing rate log (MFR): hypothesis tests for the significance of each of the fixed effects considered

Effect	Num DF	Den DF	F Value	Pr > F
Area	1	560	0.21	0.6460
StimCond	2	560	10.19	<**0.0001**
StimCond*Area	1	560	33.86	<**0.0001**
Time	3	560	34.91	<**0.0001**
StimCond*Time	6	560	23.68	<**0.0001**
Area*Time	3	560	9.51	<**0.0001**
StimCond*Area*Time	3	560	9.74	<**0.0001**

Note. Type 3 tests of fixed effects.

Due to firing rate variability typically observed among different animals, as well as temporal fluctuations in firing rates in anaesthetized preparations, it was important to examine multiple poststimulation basal periods in each animal. This approach provided not only greater statistical power but also allowed us to examine cumulative changes in firing rate in successive basal periods. In control (CTRL) experiments, no significant differences were found in MFR between any of the basal periods (Fig. 2*B* and Table 3). In contrast, MFR was significantly increased in five of six RS and six of six ADS basal period comparisons. The only exception was the Basal3 versus Basal0 comparison for RS in BF.

Table 3 Results of the general linear mixed effects model on the logarithmic firing rate log (MFR): differences of least squares means (the marginal means are estimated over a balanced population). Significant *P* values are highlighted in bold. Note that for the control experiments (CTRL), we implanted a stimulating electrode in FL, but no stimulation was delivered

Effect	Stim	Area	Time (basal)	Estimate	Std. error	*P* value
StimCond	RS versus ADS			0.56	0.18	**0.0019**
Area		BF versus FL		1.80	0.33	<**0.0001**
StimCond*Area*Time	CTRL	FL	1 versus 0	−0.12	0.20	0.542
			2 versus 0	−0.18	0.21	0.394
			3 versus 0	−0.10	0.22	0.638
	ADS	BF	1 versus 0	1.23	0.11	<**0.0001**
			2 versus 0	1.39	0.13	<**0.0001**
			3 versus 0	1.97	0.14	<**0.0001**
		FL	1 versus 0	1.05	0.16	<**0.0001**
			2 versus 0	0.51	0.16	**0.002**
			3 versus 0	1.05	0.19	<**.0001**
	RS	BF	1 versus 0	0.47	0.18	**0.0097**
			2 versus 0	0.84	0.19	<**0.0001**
			3 versus 0	0.25	0.20	0.2169
		FL	1 versus 0	1.61	0.15	<**0.0001**
			2 versus 0	1.49	0.16	<**0.0001**
			3 versus 0	1.20	0.17	<**0.0001**
	ADS versus CTRL	BF	0	−1.11	0.33	**0.0007**
		FL		034	0.36	0.3464
		BF	1	0.24	0.28	0.3868
		FL		1.51	0.30	<**0.0001**
		BF	2	0.45	0.29	0.1177
		FL		1.02	0.31	**0.0010**
		BF	3	0.96	0.30	**0.0013**
		FL		1.49	0.33	<**.0001**
	RS versus CTRL	BF	0	1.24	0.38	**0.0011**
		FL		−0.57	0.35	0.1095
		BF	1	1.82	0.32	<**0.0001**
		FL		1.17	0.30	**0.0001**
		BF	2	2.26	0.33	<**0.0001**
		FL		1.10	0.31	**0.0004**
		BF	3	1.59	0.34	<**0.0001**
		FL		0.74	0.32	**0.0214**
	RS versus ADS	BF	0	2.35	0.30	<**0.0001**
		FL		−0.90	0.31	**0.0036**

It is important to note that both ADS and RS generally induced a significant increase in firing rate in subsequent basal periods with respect to control experiments, regardless of any observed differences. As reported in Table 3 (cf. Table 3, StimCond*Area*Time, ADS/RS vs. CTRL), in the ADSBF group, MFR was significantly lower than in the CTRL group during Basal 0 but showed significantly higher MFR compared with CTRL in Basal3. For the ADSFL group, there were no significant differences with the CTRL group in Basal 0 but a significantly higher MFR in each of the subsequent basal phases. For the RSBF group, MFR was higher than the CTRL group for each the basal periods, while RSFL demonstrated a comparable MFR with respect to CTRL in Basal 0 but showed significant greater values for each of the subsequent phases. When considering the Effect "Area," the stimulation of BF was more effective in increasing firing rate than the FL (cf. Table 3, Area, BF vs. FL).

A table containing all the combinations of the third-order interaction StimCond*Area*Time is reported in the Supplementary Material section (cf. Supplementary Table S1).

We also calculated the proportion of units (i.e., neurons) whose firing rates significantly increased, decreased, or remained constant after the stimulation protocol (i.e., Basal1, Basal2, and Basal3) with respect to the initial basal period of recordings (i.e., Basal0, Fig. 3A,B). Both stimulation conditions induced a significantly greater proportion of units that showed increased firing rates across basal periods (Fig. 3C) compared with the control group. No differences were observed in the proportion of units showing a decrease in MFR in the stimulation (Fig. 3D) versus the control experiments.

Overall, these resultsl? demonstrate that, notwithstanding possible initial differences in MFR among groups, both RS and ADS stimulation conditions significantly increased the MFR of neurons recorded from RFA in the post-ICMS basal periods with respect to the initial basal period. ADS consistently showed an increase in MFR over time, in contrast to RS which showed an increase in MFR, but not for all of the experimental conditions and in sharp contrast to CTRL which never exhibited an increase in MFR. Increased MFR was accompanied by an increase in the

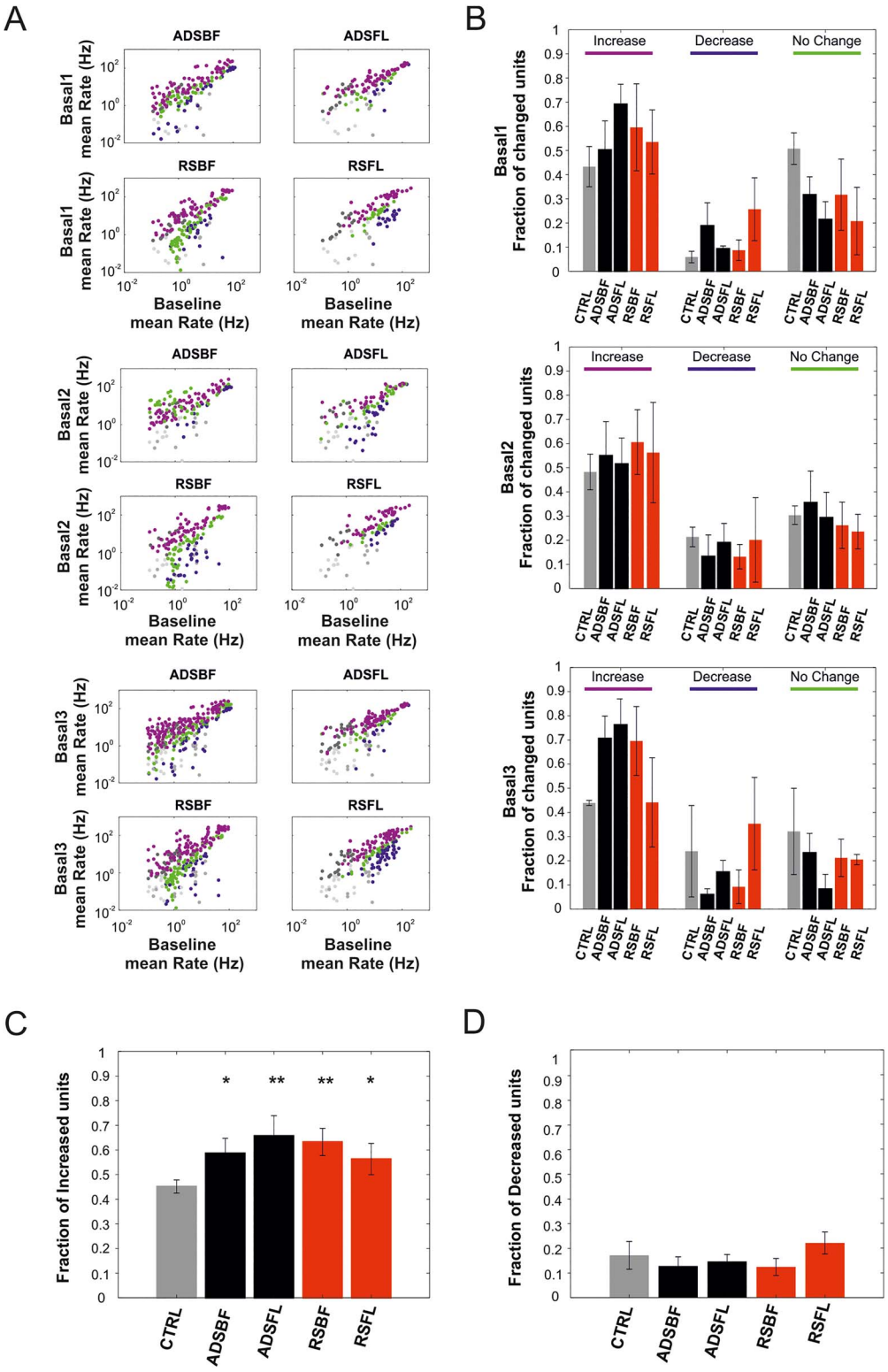

Figure 3. (*A*) Per unit correlation between baseline firing rates (*x*-axis, Basal0) and firing rates after each stimulation session (*y*-axis, Basal1–3) calculated for each group (ADSBF, ADSFL, RSBF, and RSFL). Colors represent units that significantly increased (magenta), decreased (blue), or remained stable (green). Gray dots represent the correlation for the control group (CTRL). (*B*) Average fraction of units that significantly changed their firing with respect to the baseline period of recording (Basal0) calculated for all the five experimental groups (i.e., CTRL, light gray; ADSBF and ADSBF, black; RSBF and RSFL, red). (*C*) Average fraction of neurons which increased their firing rate across the five experimental groups. (*D*) Total fraction of neurons which decreased their firing rate. (*$P < 0.05$, relative to CTRL; one-way ANOVA with Dunnett's multiple comparison test. Error bars represent SEM). Data are reported as mean ± SEM (standard error of the mean).

Table 4 Results of general linear mixed effects model on LvR: hypothesis tests for the significance of each of the fixed effects considered

Effect	Num DF	Den DF	F Value	Pr > F
Area	1	497	3.87	**0.0497**
StimCond	2	497	0.39	0.6798
StimCond*Area	1	497	0.63	0.4295
Time	3	497	20.51	<**0.0001**
StimCond*Time	6	497	3.91	**0.0008**
Area*Time	3	497	7.19	<**0.0001**
StimCond*Area*Time	3	497	2.05	0.1057

Note. Type 3 tests of fixed effects.

proportion of units with increased firing rates in both RS and ADS stimulation conditions.

ICMS Modulates Neuronal Firing Patterns in a Distant Cortical Area

We used the LvR coefficient (Fig. 4A, cf. Methods), a metric of local variation of the ISI, to "classify" the type of spike-firing pattern (e.g., "Bursty," "Random," and "Regular") of the recorded neurons in RFA during spontaneous activity. The purpose of this analysis was to understand whether the different ICMS stimulation conditions in the two areas affected spike-firing patterns. LvR distribution of neurons exhibited stable baseline firing patterns, with LvR values between "Random" and "Bursty" states (cf. Fig. 4B, ADSBF in Basal0, dotted line: LvR = 1.27 ± 0.24, mean ± SD).

Table 4 contains the results of hypothesis tests for each of the considered fixed effects. It shows that the effect "StimCond" and the combinations "StimCond*Area" and "StimCond*Area*Time" were not significant. The global effect "Area" reached significance ($P = 0.0497$), while "Time" and the other interactions were clearly significant.

No statistical difference was found for LvR values comparing the two stimulation conditions (cf. Table 5, Effect "StimCond," ADS vs. RS). The contrast between FL and BF indicates that there were no significant differences between the two stimulated somatosensory areas (Table 5, Effect "Area," BF vs. FL). Table 5 also reports how both ADS and RS altered the firing patterns across time. As expected, LvR was not affected in the CTRL experiments (Fig. 4C–E and Table 5, StimCond*Area*Time CTRL). The main result is that ICMS, either RS or ADS, generally induced a strong decrease in LvR, moving activity from the "Bursty" condition during Basal 0 towards the "Random" state of firing in the last basal period (Fig. 4B, ADSBF in Basal3, dotted line: LvR = 1.07 ± 0.02, mean ± SD and Fig. 4D,E, Table 5). This effect was observed in five of six basal period comparisons using RS and six of six basal period comparisons using ADS. The one exception was that no change in LvR was observed between Basal3 and Basal0 in the RSFL group (Table 5).

As was observed for MFR, there were differences between groups in LvR even during the initial basal period (Basal0). However, the significant changes that occurred in LvR in the post-ICMS basal periods invariably were decreases. For example, ADSBF LvR was significantly higher than CTRL during Basal 0, but this difference disappeared in Basal1. ADSBF showed a significantly lower LvR than the CTRL in Basal2 and Basal3, indicating an overall decrease of LvR for ADSBF group with respect to CTRL. LvR in the ADSFL group was significantly higher than the CTRL in Basal0, but the difference disappeared in all subsequent basal phases. The RSBF group was higher than the CTRL in Basal0, but the difference disappeared in Basal1 and Basal2. Finally, RSBF was significantly lower than CTRL during Basal3. RSFL was found to be not statistically different from CTRL in any of the basal periods.

A table containing all of the combinations of the effect StimCond*Area*Time is reported in the Supplementary Material section (cf. Table S2).

RS and ADS Exhibit Different Effects on Stimulus-Associated Action Potentials in a Distant Cortical Area

Evoked action potentials (in RFA) in response to ICMS were analyzed by discriminating the spiking activity in the 28 ms after each S1FL or S1BF stimulus pulse using PSTH (cf. Methods). Due to differences in the dynamics of the evoked electrical artifacts in different animals, we used an adaptive-length blanking window (from 4 to 6 ms, Fig. 5A). As shown in Fig. 5B, the interstimulus intervals (ISIs) used for the RS groups comprised a range of values comparable to those of the ADS groups. Interestingly, the ISI distribution for ADS was stable over repeated stimulation trials (cf. Fig. 5B, left). There was, however, a bias toward ~200-ms interstimulus intervals in the ADS group, whereas the RS intervals exponentially decreased across the range (Fig. 5B).

Table 6 contains the results of hypothesis tests for each of the considered fixed effects. It indicates that the effects "Area," "Time," and their interactions induced significant changes in the evoked activity. However, the fixed effect "StimCond," which includes the contribution of "Area" and "Time" and does not capture each effect singularly (cf. Effect StimCond*Area*Time for a more specific description), was not significant (cf. Table 6, Effect "StimCond").

Our analysis indicated that ICMS in BF was significantly more effective in evoking short-latency spikes (<28 ms) than in FL (Table 7, Effect "Area," BF vs. FL). Examining differences between the two stimulation conditions, it appeared that ADS had a more consistent, cumulative effect in eliciting evoked spikes over time (cf. Table 7, Effect StimCond*Area*Time, ADS, both BF and FL). This is evident in Figure 5C,D, showing a progressive increase in short-latency spike counts and PSTH area, respectively, in ADS. Changes in evoked spike activity with RS were smaller and inconsistent. Statistically significant differences between RS and ADS were found in three of three of the FL stim period comparisons and two of three BF stim period comparisons (Table 7).

Regarding the stimulus location, we observed that ADSFL consistently evoked more poststimulus spikes than RSFL. A table

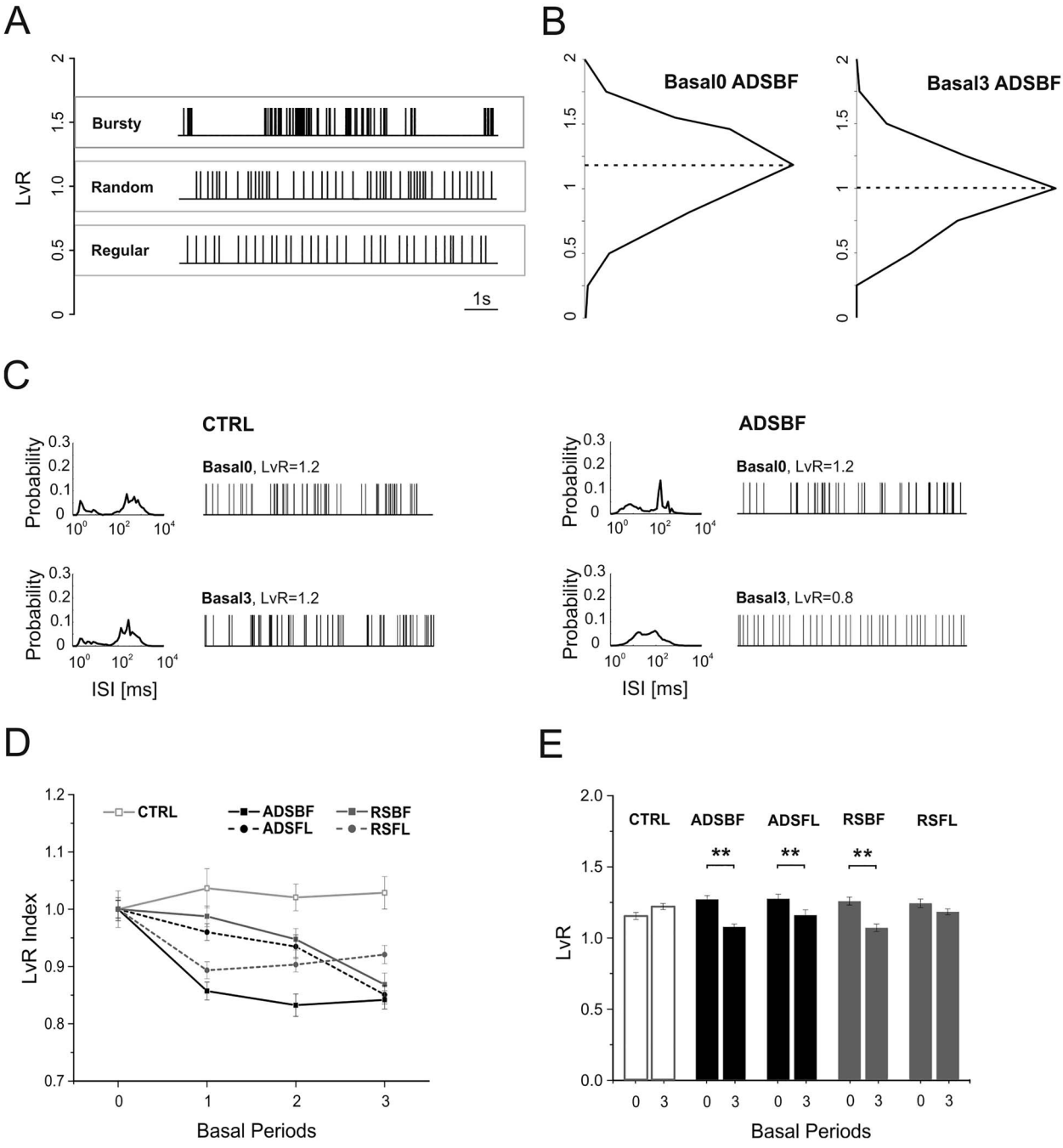

Figure 4. (*A*) Example spike sequences of representative neurons with LvR of 0.5 (Regular, red), 1 (Random, green), and 1.5 (Bursty, blue) taken from data set ADSBF. (*B*) LvR distributions shown as histograms with a common bin size 0.25 and determined across all the subjects belonging from ADSBF during the first (Basal0, left) and last (Basal3, right) period of quiescence. Black dotted lines represent the median of the LvR distributions. (*C*) Distributions of a representative neuron's ISI and its sample firing pattern consisting of 100 consecutive ISIs belonging to the CTRL group (Left) and ADSBF group (right), respectively, during Basal0 (top) and Basal3 (bottom). (*D*) Mean ± SEM trend of normalized LvR for each experimental condition. Each subject's LvR value was normalized over the mean LvR value calculated during Basal0: statistical analysis is reported in Tables 4 and 5. (*E*) Mean ± SEM LvR comparison between Basal0 and Basal3 for all the experimental conditions (CTRL, grey; ADSBF and ADSFL, black; RSBF and RSFL, red). $^{**}P < 0.01$; unpaired, two-tailed Student's *t*-test.

containing all the combinations of the effect StimCond*Area*Time is reported in the Supplementary Material section (cf. Supplementary Table S3).

Since both ICMS protocols induced a nonspecific increase of firing rate with respect to nonstimulated animals (cf. Fig. 2) during the basal periods following the stimulation (Basal1, Basal2, and Basal3), we investigated the level of firing rate and the changes occurring during the three stimulation phases (Stim1, Stim2, and Stim3). We found that, although the number of pulses delivered by ADS was stable and lower than RS during the entire treatment (cf. Fig. 5E), ADS of BF incrementally increases the overall firing rate of the recorded RFA's activity with respect to RS

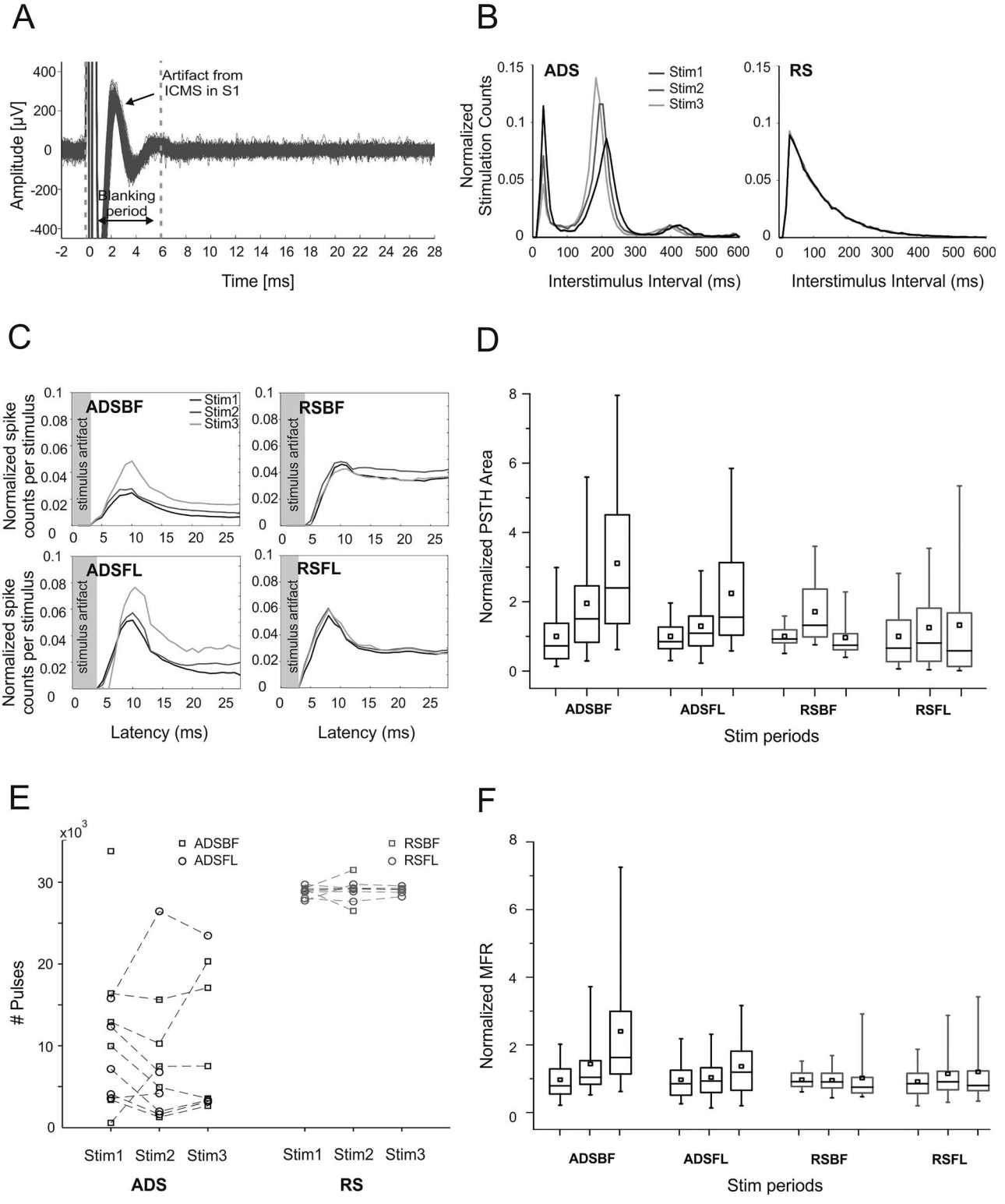

Figure 5. (*A*) Sample trace of recordings from RFA showing stimulus artifacts from ICMS delivered to S1BF. Blanking period used for the analysis is delimited by the gray dotted lines. A total of 100 superimposed traces are shown. (*B*) Stimulation interval distribution (Interstimulus intervals, 600 ms) in both one ADS and RS subject during the three stimulation sessions (Stim1, Stim2, and Stim3). Stimulation counts have been normalized to session length. (*C*) Poststimulus spiking histograms derived from neural recordings in RFA on the three stimulation sessions for the four ICMS groups, respectively (ADSBF, ADSFL, RSBF, and RSFL). Histograms portray the average number of action potentials discriminated from the neural recordings within 1-ms bin. Data pooled across subjects for each group and normalized to the total number of either ADS or RS specific events. (*D*) Normalized PSTH areas for the four groups (ADSBF and ADSFL, black; RSBF and RSFL, red) of ICMS in the three stimulation phases (Stim1, Stim2, and Stim3). Each subject's PSTH area was normalized over the mean area calculated in Basal0 to show data trends over time. (*E*) The number of stimulation pulses delivered for both ADS (black) and RS (red) during the three stimulation phases. (*F*) MFR of the stimulation phases normalized over the mean value of firing during Stim1. Statistical analysis is reported in Tables 6–9.

Table 5 Results of general linear mixed effects model on LvR: differences of least squares means (the marginal means are estimated over a balanced population).

Effect	StimCond	Area	Time (basal)	Estimate	Std. error	*P* value
StimCond	ADS versus RS			0.02	0.02	0.3819
Area		BF versus FL		0.01	0.04	0.7259
StimCond*Area*Time	CTRL	FL	1 versus 0	0.02	0.03	0.550
			2 versus 0	0.03	0.03	0.377
			3 versus 0	0.07	0.03	0.054
	ADS	BF	1 versus 0	−0.14	0.02	**<0.0001**
			2 versus 0	−0.18	0.03	**<0.0001**
			3 versus 0	−0.20	0.24	**<0.0001**
		FL	1 versus 0	−0.08	0.03	**0.003**
			2 versus 0	−0.12	0.03	**0.0001**
			3 versus 0	−0.11	0.03	**0.0003**
	RS	BF	1 versus 0	−0.14	0.28	**<0.0001**
			2 versus 0	−0.15	0.03	**<0.0001**
			3 versus 0	−0.19	0.03	**<0.0001**
		FL	1 versus 0	−0.14	0.03	**<0.0001**
			2 versus 0	−0.12	0.03	**0.0001**
			3 versus 0	−0.06	0.03	0.051
	ADS versus CTRL	BF	0	0.12	0.04	**0.0045**
		FL		0.12	0.04	**0.0063**
		BF	1	−0.04	0.35	0.2511
		FL		0.02	0.04	0.5923
		BF	2	−0.09	0.04	**0.0113**
		FL		−0.03	0.04	0.4936
		BF	3	−0.15	0.33	**<0.0001**
		FL		−0.06	0.04	0.1100
	RS versus CTRL	BF	0	0.10	0.04	**0.0183**
		FL		0.09	0.05	0.0504
		BF	1	−0.06	0.04	0.1343
		FL		−0.07	0.04	0.0989
		BF	2	−0.07	0.04	0.0588
		FL		−0.07	0.04	0.0912
		BF	3	−0.15	0.04	**<0.0001**
		FL		−0.04	0.04	0.3115
	RS versus ADS	BF	0	−0.01	0.04	0.7400
		FL		−0.17	0.04	**<0.0001**

Note. Significant *P* values are highlighted in bold.

Table 6 Results of general linear mixed effects model on PSTH: hypothesis tests for the significance of each of the fixed effects considered

Effect	Num DF	Den DF	F Value	Pr > F
Area	1	299	16.71	**<0.0001**
StimCond	1	299	0.10	0.7469
StimCond*Area	1	299	45.42	**<0.0001**
Time	2	299	30.73	**<0.0001**
StimCond*Time	2	299	17.58	**0.0008**
Area*Time	2	299	16.55	**<0.0001**
StimCond*Area*Time	2	299	3.32	**0.0375**

Note. Type 3 tests of fixed effects.

(cf. Fig. 5F, Effect StimCond*Area*Time, Area BF, Table 9) where a decrease was found. Contrarily, no differences were found for both the FL groups (cf. Effect StimCond*Area*Time, Area FL, Table 9). This result further underlies the differential effect of ADS and RS under stimulation regime, allowing the results to be extended for longer time scales (i.e., the entire duration of the stimulation phase).

ADS Increases the Coupling between the Trigger Channel and the Population in RFA

We used PC coefficient, computed as the peak of the stPR (Fig. 6A and Methods) to understand whether the properties of the triggering channel could impact the effectiveness of the ADS protocol. In our experiments, the initial levels of coupling of the

Table 7 Results of general linear mixed effects model on PSTH: differences of least squares means (the marginal means are estimated over a balanced population)

Effect	StimCond	Area	Time (Stim)	Estimate	Std. error	*P* value
StimCond	RS versus ADS			0.01	0.05	0.7469
Area		BF versus FL		0.19	0.05	<**0.0001**
StimCond*Area*Time	ADS	BF	2 versus 1	0.19	0.03	<**0.0001**
			3 versus 1	0.38	0.05	<**0.0001**
			3 versus 2	0.18	0.03	<**0.0001**
		FL	2 versus 1	0.06	0.03	**0.0263**
			3 versus 1	0.26	0.06	**0.0001**
			3 versus 2	0.21	0.04	<**0.0001**
	RS	BF	2 versus 1	0.16	0.04	<**0.0001**
			3 versus 1	0.03	0.06	0.6663
			3 versus 2	0.14	0.04	**0.0009**
		FL	2 versus 1	0.03	0.03	0.3777
			3 versus 1	0.11	0.05	**0.0358**
			3 versus 2	0.08	0.04	**0.0231**
	RS versus ADS	BF	1	0.45	0.07	<**0.0001**
		FL		−0.23	0.07	**0.0005**
		BF	2	0.42	0.06	<**0.0001**
		FL		−0.26	0.06	<**0.0001**
		BF	3	0.10	0.09	0.2527
		FL		−0.39	0.09	<**0.0001**

Note. Significant *P* values are highlighted in bold.

Table 8 Results of general linear mixed effects model on MFR during Stim: hypothesis tests for the significance of each of the fixed effects considered

Effect	Num DF	Den DF	*F* Value	Pr > F
Area	1	300	63.76	<**0.0001**
StimCond	1	300	25.13	<**0.0001**
StimCond*Area	1	300	31.27	<**0.0001**
Time	2	300	5.58	**0.0042**
StimCond*Time	2	300	22.93	<**0.0001**
Area*Time	2	300	0.55	0.5773
StimCond*Area*Time	2	300	16.40	<**0.0001**

Note. Type 3 tests of fixed effects.

Table 9 Results of general linear mixed effects model on MFR during Stim: differences of least squares means (the marginal means are estimated over a balanced population)

Effect	StimCond	Area	Time (Stim)	Estimate	Std. error	*P* value
StimCond	RS versus ADS			−7.35	1.47	<**0.0001**
Area		BF versus FL		11.7	1.47	<**0.0001**
StimCond*Area*Time	ADS	BF	2 versus 1	2.01	0.91	**0.0271**
			3 versus 1	11.21	1.67	<**0.0001**
			3 versus 2	9.20	1.14	<**0.0001**
		FL	2 versus 1	0.68	0.91	0.4540
			3 versus 1	2.61	1.88	0.1674
			3 versus 2	1.93	1.43	0.1790
	RS	BF	2 versus 1	2.06	1.82	0.0695
			3 versus 1	−4.57	2.04	**0.0258**
			3 versus 2	−6.64	1.44	<**0.001**
		FL	2 versus 1	1.46	1.02	0.1523
			3 versus 1	2.35	1.87	0.2093
			3 versus 2	0.90	1.27	0.4823
	RS versus ADS	BF	1	20.79	1.85	<**0.0001**
		FL		−1.02	1.85	0.5816
		BF	2	20.84	2.01	<**0.0001**
		FL		0.24	2.06	0.9054
		BF	3	5	3.04	0.1009
		FL		1.28	3.12	0.6824

Note. Significant *P* values are highlighted in bold.

trigger channels with the rest of the network varied from high (Choristers) to weak (Soloists) levels of coupling, with no particular tendency for any one of them (Fig. 6B). Specifically, our analysis indicated that four Choristers (two for ADSBF, two for ADSFL) and four Soloists (two for ADSBF, two for ADSFL) were chosen for triggering the stimulation (four additional trigger channels were not classified). The distribution of the PC values during Basal0 was computed for all the electrodes of the network and spanned from high to low values as for the triggering channels (Fig. 6B, ADSBF and ADSFL).

We then checked whether the PC values changed in the course of the experiments (Fig. 6C). We found that ICMS stimulation, either ADS or RS, did not influence the strength of coupling with the population for all the recorded channels. The sites selected for triggering the stimulation, on the contrary, showed an incremental increase of their correlation with the population activity following ADS, resulting in a significant change of their strength during all the stimulation phases (Stim1, Stim2, and Stim3) and at the end of the treatment (i.e., Basal3, Fig. 6C).

Discussion

For several decades, electrical microstimulation has been an important tool for investigating neural circuits, demonstrating evidence of cortical map plasticity, and for therapeutic neuromodulation (Benali et al. 2008; Buonomano and Merzenich 1998; De Hemptinne et al. 2015). Despite its widespread use, our understanding of its effects beyond local depolarization of neuronal membranes remains limited. While the behavioral outcomes of microstimulation in sensory and motor regions of the brain have been characterized extensively (Cheney et al. 2013; Overstreet et al. 2013), few studies have examined the long-term effects of repetitive microstimulation on neuronal activity in the broader network of interconnected brain regions (Nudo et al. 1990). Those that have examined distant effects of microstimulation have focused primarily on the alteration in neuronal activity in primary motor cortex (M1) induced by the stimulation of the subthalamic nucleus (STN) as a model to understand the effects of DBS therapy in Parkinson's disease (De Hemptinne et al. 2013; De Hemptinne et al. 2015; Kuriakose et al. 2009; Li et al. 2012; McCairn and Turner 2015). As adaptive, or closed-loop, microstimulation modalities are increasingly being explored as potential options for therapeutic applications (Guggenmos et al. 2013; Meidahl et al. 2017), it is important to understand how various stimulation patterns differentially alter both spontaneous and stimulus-evoked neuronal activity in interconnected regions of the brain.

The specific aim of the present work was to characterize the neurophysiological effects of random and activity-dependent ICMS on healthy cortical networks. Indeed, our study indicates ICMS is able to alter, within hours, the firing characteristics within a distant, but connected, cortical area (RFA).

In a previous study, we demonstrated that ADS triggered by spikes in RFA and applied to S1 resulted in a rapid improvement in motor skill in a traumatic brain injury model in rats (Guggenmos et al. 2013). The effects of ADS were substantially greater than those of open-loop stimulation. While the underlying mechanisms for recovery were thought to depend upon altered synaptic efficacy between the two regions in the ADS condition, the time course of and regional specificity of the effect are largely unknown. To determine the impact of ADS

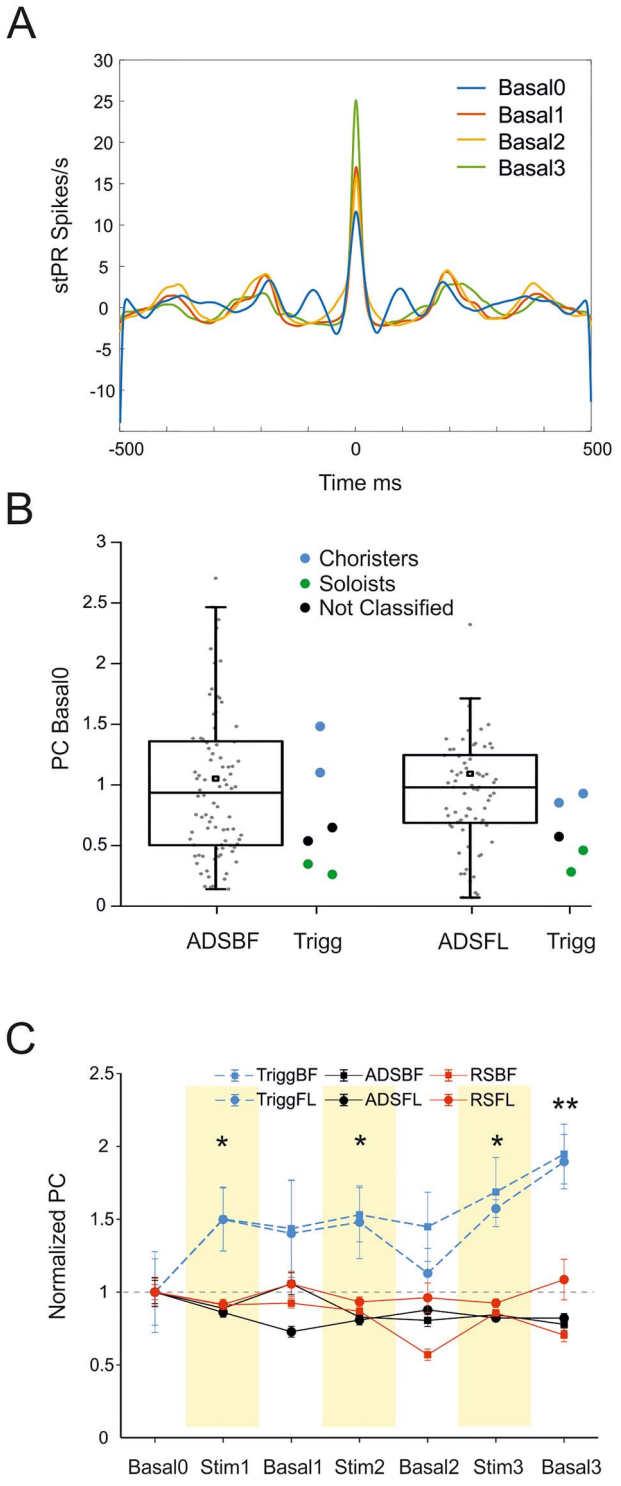

Figure 6. (A) stPR for a representative trigger channel of an ADSBF experiment during the four basal periods of recording. (B) Box plots showing the initial level of PC for ADS groups during Basal0. Light blue, black, and green symbols represent the PC classification of the trigger channels, respectively, Choristers, Not Classified, and Soloists. (C) PC normalized over the mean value of Basal0 for the trigger channels groups of ADSBF, ADSFL, and all the other recording groups. *$P < 0.05$, **$P < 0.001$, one-way repeated measures analysis of variance (ANOVA) on ranks, Dunnett's post hoc testing procedure.

on distant cortical regions in healthy anesthetized rats within single recording sessions, we applied either randomized ICMS (i.e., open-loop) or activity-triggered ICMS (i.e., closed-loop) to one of two somatosensory cortical areas (forelimb or BF) while recording resultant neuronal activity in the RFA, a premotor cortical area. These regions were chosen due to their known intracortical connections and our ability to alter synaptic efficacy in the target pathways in a previous study (Guggenmos et al. 2013). We found that ICMS in somatosensory areas induced an increase in spontaneous firing rates in RFA when compared with nonstimulated controls (Figs 2 and 3, Table 3). Furthermore, we observed a reduction in the LvR values, indicating a shift towards more random ISIs of recorded units within RFA (Fig. 4E, Table 5). Finally, we found an increase in the stimulus-evoked activity in RFA (Fig. 5, Tables 6 and 7). While both forms of stimulation-induced increases in spontaneous firing rates and decreases in LvR, effects were marginally more consistent with ADS. A more pronounced difference between the two stimulation conditions was found in the ability to evoke short-latency spikes ($\leq$28 ms) in RFA. Increases in evoked spikes as a result of ADS were progressive over multiple stimulation periods and were significantly different from the results of RS.

Both RS and ADS modulated spontaneous firing rates and patterns within RFA in a similar manner. Both resulted in decreased LvR, which was initially associated with a mixed "Random"-"Bursty" intrinsic firing pattern, indicating a shift towards a "Random" state of firing at the end of the treatment (cf. Fig. 4E). Target location had an impact on the response, as stimulating BF was more effective than FL in increasing the spontaneous firing rate in RFA (cf. Table 3, effect "Area," BF vs. FL). Examining the evoked response, stimulation from BF was also more effective in directly evoking action potentials in RFA (cf. Fig. 5C,D and Table 6, effect "Area," BF vs. FL). Anatomically, RFA has dense, reciprocal connections with CFA, and relatively sparse connections to either S1FL or S1BF, while S1FL tends to have a significantly higher number of projections to CFA than BF (Zakiewicz et al. 2014). Given the existing anatomical framework, we expected that stimulation within S1FL would have a significantly greater impact on RFA activity than S1BF stimulation as this is a stronger cortico-cortical pathway. Surprisingly, the effect was the opposite, with S1BF having a greater role in modulating RFA activity. It is possible that the efferent flow of information from CFA differs based on the input source, or that CFA acts to modulate or inhibit this activity and has less modulatory effect with the fewer projections from S1BF. Other cortical (and subcortical) structures undoubtedly contribute to the effects of repetitive microstimulation as well (cf. Fig. 1), further complicating how spiking/stimulation information is transferred through the network.

Both ICMS protocols induced changes in firing rate with respect to nonstimulated animals (CTRL) where no changes were observed. This may be a result of both the ADS and RS introducing potentially physiologically relevant inputs into the somatosensory cortex. Temporal coding is in fact, critical for enhancing the network entrainment (synaptic efficacy) (Gal and Marom 2013; Mainen and Sejnowski 1995; Scarsi et al. 2017), and either ADS or Poisson distributed stimulation may similarly enhance the intrinsic pathways that would lead to increased firing rates in spontaneous activity.

Interestingly, even if there was an initial difference between ADS and RS groups during the baseline period of recording, ADS was invariably able to increase firing rates over time, compared with RS. No differences were found in the LvR analysis (Table 5, Effect "StimCond," RS vs. ADS), but ADS more reliably displayed lowered LvR over time (cf. Table 5, Effect StimCond*Area*Time, Time 4 vs. 1 for all the groups).

More interestingly, ADS, and not RS, facilitated progressive increases of stimulus-associated activity over time (cf. Effect StimCond*Area*Time for ADS and RS in Table 7), suggesting that the pairing of neural activity and stimulation may lead to stronger associations over prolonged stimulation sessions. This may result from a number of factors including the temporal distribution of the stimuli and coordination between stimulation and neuronal activity which concern has already been raised by several studies previously (Mourão et al. 2015; Nelson et al. 2011; Popovych et al. 2017; Quinkert et al. 2010; Wyckhuys et al. 2010a; Wyckhuys et al. 2010b). It is likely that the mechanism that increases the effectiveness of ADS is through Hebbian-based spike-timing, which is a method that more closely mimics the nervous system's natural mechanism to promote learning and memory which is typically effective in inducing long-term plasticity (Guggenmos et al. 2013; Jackson et al. 2006).

Finally, sites selected for triggering the stimulation showed an initial level of coupling with the network comparable to those of the other electrodes, suggesting that the initial properties of the trigger do not have a particular influence on the outcome of the stimulation. Interestingly, trigger channels exhibited an increased PC following ADS, which was statistically significant for both the stimulus location (BF and FL) during the stimulation sessions and at the end of the treatment (i.e., Basal3, cf. Fig. 6). Generally, neurons with strong PC receive more synaptic inputs from their neighbors (Okun et al. 2015). An increase in the PC for the channels that drive the stimulation (i.e., the trigger channels) could suggest the ability of ADS to selectively increase mean synaptic input strength as a consequence of repetitive treatments.

While these studies provide important evidence for the effects of electrical microstimulation on the broader neuronal network, it is important to consider the limitations imposed by the ketamine-anesthetized preparation. An anesthetized preparation has numerous advantages for the present investigation, since the state of the animal and the associated neurophysiological set-up is relatively stable over several hours. While it is technically feasible to conduct these studies in awake, ambulatory animals, substantial variability in spike activity is introduced by the sensorimotor activities of the animals. However, ketamine is widely known as a noncompetitive N-methyl d-aspartate receptor antagonist and can modulate other receptors or channels such as the GABAa receptor. As a result, ketamine has diverse and temporally complex effects on neuronal activity (Brown et al. 2010; Brown et al. 2011; Homayoun and Moghaddam 2007). For example, under ketamine anesthesia, different cell types in the hippocampus show differential effects in firing rate and synchrony (Kuang et al. 2010). Ketamine causes enhanced gamma oscillations acutely, but decreased network gamma oscillations with chronic (Ahnaou et al. 2017) administration. Thus, while ketamine anesthesia undoubtedly had some effect on neuronal firing in the present study, the changes in MFR, LvR, and evoked spikes are thought to be largely independent of the anesthetic state. This hypothesis could be tested with different anesthetics (Mahmud et al. 2016) and should be verified in awake, ambulatory animals. In further investigations, it would be beneficial to identify and understand the role of different cell types involved in the generation of spontaneous activity, as it has been reported that the frequency and amplitude of the stimulation can differentially modulate excitatory and

inhibitory neurons (Mahmud et al. 2016; Mahmud and Vassanelli 2016).

In summary, RS and ADS protocols both induce changes in the recorded activity in RFA. Focal electrical stimulation has the ability to alter activity in remote brain regions not directly influenced by the current spread from the electrode. The closed-loop condition (ADS) is more able to alter evoked responses and thus modulate cortico-cortical connectivity in the rat brain within a single recording period. Closed-loop stimulation for therapeutic applications in the human brain is rare, but there is a common interest for brain-inspired implantable devices aimed at the rehabilitation or augmentation of brain functions (Mahmud et al. 2017; Vassanelli and Mahmud 2016; Vassanelli et al. 2012). Similar approaches are already being tested for epilepsy, in Parkinson disease and in animal models of spinal cord injury (Jackson and Zimmermann 2012; Nishimura et al. 2013b; Santos et al. 2011; Skarpaas and Morrell 2009). Other potential clinical applications based on closed-loop ICMS treatments include stroke, focal TBI, and surgical resections. Although the beneficial effect of these approaches in humans is still not clear, we propose that ADS could be used to modulate cortical state and connectivity by steering neuroplasticity after injury. Additional studies need to be performed to determine the precise parameters and characteristics related to these alterations.

Supplementary Material

Supplementary material is available at *Cerebral Cortex* online.

Funding

Italian Ministry of Foreign Affairs and International Collaboration (MAECI); Directorate General for Country Promotion, as a high-relevance bilateral project within the Italy–USA; National Institutes of Health (grants R01NS030853, R03HD094608).

Notes

The authors thank Giacomo Siri from the University of Genova for his support in the statistical model development and Caleb Dunham from the University of Kansas Medical Center for technical assistance with spike analysis and data management.

Conflicts of Interest: None declared.

Author Contributions

A.A., R.J.N., M.C., and D.G. designed the study. A.A., G.V.A., M.M., and D.G. performed the experiments. A.A., V.P., M.M., and M.C. designed the pipeline for the data analysis. AA performed the analysis. A.A., M.P.R., and V.P. performed the statistical analysis. A.A., M.C., D.G., and R.J.N. wrote the paper. All the authors have read and approved the manuscript.

References

Ahnaou A, Huysmans H, Biermans R, Manyakov N, Drinkenburg W. 2017. Ketamine: differential neurophysiological dynamics in functional networks in the rat brain. *Transl Psychiatry*. 7(9):e1237.

Anderson VC, Burchiel KJ, Hogarth P, Favre J, Hammerstad JP. 2005. Pallidal vs subthalamic nucleus deep brain stimulation in Parkinson disease. *Arch Neurol*. 62(4):554–560.

Benali A, Weiler E, Benali Y, Dinse HR, Eysel UT. 2008. Excitation and inhibition jointly regulate cortical reorganization in adult rats. *J Neurosci*. 28(47):12284–12293.

Berg J, Dammann J III, Tenore F, Tabot G, Boback J, Manfredi L, Peterson M, Katyal K, Johannes M, Makhlin A. 2013. Behavioral demonstration of a somatosensory neuroprosthesis. *IEEE Trans Neural Syst Rehabil Eng*. 21(3):500–507.

Blatt M, Wiseman S, Domany E. 1996. Superparamagnetic clustering of data. *Phys Rev Lett*. 76(18):3251.

Bradley DC, Troyk PR, Berg JA, Bak M, Cogan S, Erickson R, Kufta C, Mascaro M, McCreery D, Schmidt EM. 2005. Visuotopic mapping through a multichannel stimulating implant in primate V1. *J Neurophysiol*. 93(3):1659–1670.

Bronstein JM, Tagliati M, Alterman RL, Lozano AM, Volkmann J, Stefani A, Horak FB, Okun MS, Foote KD, Krack P. 2011. Deep brain stimulation for Parkinson disease: an expert consensus and review of key issues. *Arch Neurol*. 68(2):165–165.

Brown EN, Lydic R, Schiff ND. 2010. General anesthesia, sleep, and coma. *N Engl J Med*. 363(27):2638–2650.

Brown EN, Purdon PL, Van Dort CJ. 2011. General anesthesia and altered states of arousal: a systems neuroscience analysis. *Annu Rev Neurosci*. 34:601–628.

Buonomano DV, Merzenich MM. 1998. Cortical plasticity: from synapses to maps. *Annu Rev Neurosci*. 21(1):149–186.

Chen KH, Dammann JF, Boback JL, Tenore FV, Otto KJ, Gaunt RA, Bensmaia SJ. 2014. The effect of chronic intracortical microstimulation on the electrode–tissue interface. *J Neural Eng*. 11(2):026004.

Cheney P, Griffin D, Van Acker IIIG. 2013. Neural hijacking: action of high-frequency electrical stimulation on cortical circuits. *Neuroscientist*. 19(5):434–441.

Cohen MR, Newsome WT. 2004. What electrical microstimulation has revealed about the neural basis of cognition. *Curr Opin Neurobiol*. 14(2):169–177.

Davis T, Parker R, House P, Bagley E, Wendelken S, Normann R, Greger B. 2012. Spatial and temporal characteristics of V1 microstimulation during chronic implantation of a microelectrode array in a behaving macaque. *J Neural Eng*. 9(6):065003.

De Hemptinne C, Ryapolova-Webb ES, Air EL, Garcia PA, Miller KJ, Ojemann JG, Ostrem JL, Galifianakis NB, Starr PA. 2013. Exaggerated phase–amplitude coupling in the primary motor cortex in Parkinson disease. In: *Proceedings of the National Academy of Sciences*. 110(12):4780–4785.

De Hemptinne C, Swann NC, Ostrem JL, Ryapolova-Webb ES, San Luciano M, Galifianakis NB, Starr PA. 2015. Therapeutic deep brain stimulation reduces cortical phase-amplitude coupling in Parkinson's disease. *Nat Neurosci*. 18(5):779.

Deuschl G, Schade-Brittinger C, Krack P, Volkmann J, Schäfer H, Bötzel K, Daniels C, Deutschländer A, Dillmann U, Eisner W. 2006. A randomized trial of deep-brain stimulation for Parkinson's disease. *N Engl J Med*. 355(9):896–908.

Dobelle W, Mladejovsky M. 1974. Phosphenes produced by electrical stimulation of human occipital cortex, and their application to the development of a prosthesis for the blind. *J Physiol*. 243(2):553–576.

Fisher R, Salanova V, Witt T, Worth R, Henry T, Gross R, Oommen K, Osorio I, Nazzaro J, Labar D. 2010. Electrical stimulation of the anterior nucleus of thalamus for treatment of refractory epilepsy. *Epilepsia*. 51(5):899–908.

Fox MD, Buckner RL, Liu H, Chakravarty MM, Lozano AM, Pascual-Leone A. 2014. Resting-state networks link invasive and noninvasive brain stimulation across diverse psychi-

atric and neurological diseases. *Proc Natl Acad Sci*. 111(41): E4367–E4375.

Gal A, Marom S. 2013. Entrainment of the intrinsic dynamics of single isolated neurons by natural-like input. *J Neurosci*. 33(18):7912–7918.

Guggenmos DJ, Azin M, Barbay S, Mahnken JD, Dunham C, Mohseni P, Nudo RJ. 2013. Restoration of function after brain damage using a neural prosthesis. *Proc Natl Acad Sci U S A*. 110(52):21177–21182.

Harville DA. 1977. Maximum likelihood approaches to variance component estimation and to related problems. *J Am Stat Assoc*. 72(358):320–338.

Histed MH, Ni AM, Maunsell JH. 2013. Insights into cortical mechanisms of behavior from microstimulation experiments. *Prog Neurobiol*. 103:115–130.

Homayoun H, Moghaddam B. 2007. NMDA receptor hypofunction produces opposite effects on prefrontal cortex interneurons and pyramidal neurons. *J Neurosci*. 27(43):11496–11500.

Jackson A, Mavoori J, Fetz EE. 2006. Long-term motor cortex plasticity induced by an electronic neural implant. *Nature*. 444(7115):56–60.

Jackson A, Zimmermann JB. 2012. Neural interfaces for the brain and spinal cord—restoring motor function. *Nat Rev Neurol*. 8(12):690.

Kerrigan JF, Litt B, Fisher RS, Cranstoun S, French JA, Blum DE, Dichter M, Shetter A, Baltuch G, Jaggi J. 2004. Electrical stimulation of the anterior nucleus of the thalamus for the treatment of intractable epilepsy. *Epilepsia*. 45(4):346–354.

Kleim JA, Barbay S, Nudo RJ. 1998. Functional reorganization of the rat motor cortex following motor skill learning. *J Neurophysiol*. 80(6):3321–3325.

Kleim JA, Bruneau R, VandenBerg P, MacDonald E. 2003. Motor cortex stimulation enhances motor recovery and reduces peri-infarct dysfunction following ischemic insult. *Neurol Res*. 25(8):789–793.

Kuang H, Lin L, Tsien JZ. 2010. Temporal dynamics of distinct CA1 cell populations during unconscious state induced by ketamine. *PLoS One*. 5(12):e15209.

Kuriakose R, Saha U, Castillo G, Udupa K, Ni Z, Gunraj C, Mazzella F, Hamani C, Lang AE, Moro E. 2009. The nature and time course of cortical activation following subthalamic stimulation in Parkinson's disease. *Cereb Cortex*. 20(8):1926–1936.

Lee K, Jang K, Shon Y. 2006. Chronic deep brain stimulation of subthalamic and anterior thalamic nuclei for controlling refractory partial epilepsy. *Advances in functional and reparative neurosurgery*. Springer: Vienna, 87–91.

Li Q, Ke Y, Chan DC, Qian Z-M, Yung KK, Ko H, Arbuthnott GW, Yung W-H. 2012. Therapeutic deep brain stimulation in Parkinsonian rats directly influences motor cortex. *Neuron*. 76(5):1030–1041.

Little S, Pogosyan A, Neal S, Zavala B, Zrinzo L, Hariz M, Foltynie T, Limousin P, Ashkan K, FitzGerald J. 2013. Adaptive deep brain stimulation in advanced Parkinson disease. *Ann Neurol*. 74(3):449–457.

Maccione A, Gandolfo M, Massobrio P, Novellino A, Martinoia S, Chiappalone M. 2009. A novel algorithm for precise identification of spikes in extracellularly recorded neuronal signals. *J Neurosci Methods*. 177(1):241–249.

Mahmud M, Cecchetto C, Maschietto M, Thewes R, Vassanelli S. 2017. Towards high-resolution brain-chip interface and automated analysis of multichannel neuronal signals. In: *2017 IEEE Region 10 Humanitarian Technology Conference (R10-HTC)*. New York: IEEE, pp. 868–872.

Mahmud M, Cecchetto C, Vassanelli S. 2016. An automated method for characterization of evoked single-trial local field potentials recorded from rat barrel cortex under mechanical whisker stimulation. *Cogn Comput*. 8(5):935–945.

Mahmud M, Vassanelli S. 2016. Differential modulation of excitatory and inhibitory neurons during periodic stimulation. *Front Neurosci*. 10:62.

Mainen ZF, Sejnowski TJ. 1995. Reliability of spike timing in neocortical neurons. *Science*. 268(5216):1503–1506.

McCairn KW, Turner RS. 2015. Pallidal stimulation suppresses pathological dysrhythmia in the parkinsonian motor cortex. *J Neurophysiol*. 113(7):2537–2548.

Meidahl AC, Tinkhauser G, Herz DM, Cagnan H, Debarros J, Brown P. 2017. Adaptive deep brain stimulation for movement disorders: the long road to clinical therapy. *Mov Disord*. 32(6):810–819.

Mohammed H, Jain N. 2016. Ipsilateral cortical inputs to the rostral and caudal motor areas in rats. *J Comp Neurol*. 524(15):3104–3123.

Morrell MJ. 2011. Responsive cortical stimulation for the treatment of medically intractable partial epilepsy. *Neurology*. 77(13):1295–1304.

Mourão FAG, Lockmann ALV, Castro GP, de Castro MD, Reis MP, Pereira GS, Massensini AR, Moraes MFD. 2015. Triggering different brain states using asynchronous serial communication to the rat amygdala. *Cereb Cortex*. 26(5): 1866–1877.

Nelson TS, Suhr CL, Lai A, Halliday AJ, Freestone DR, McLean KJ, Burkitt AN, Cook MJ. 2011. Exploring the tolerability of spatiotemporally complex electrical stimulation paradigms. *Epilepsy Res*. 96(3):267–275.

Nishimura Y, Perlmutter SI, Eaton RW, Fetz EE. 2013a. Spike-timing-dependent plasticity in primate corticospinal connections induced during free behavior. *Neuron*. 80(5):1301–1309.

Nishimura Y, Perlmutter SI, Fetz EE. 2013b. Restoration of upper limb movement via artificial corticospinal and musculospinal connections in a monkey with spinal cord injury. *Frontiers in Neural Circuits*. 7:57.

Nudo R, Jenkins W, Merzenieh M. 1990. Repetitive microstimulation alters the cortical representation of movements in adult rats. *Somatosens Mot Res*. 7(4):463–483.

Okun M, Steinmetz NA, Cossell L, Iacaruso MF, Ko H, Bartho P, Moore T, Hofer SB, Mrsic-Flogel TD, Carandini M *et al*. 2015. Diverse coupling of neurons to populations in sensory cortex. *Nature*. 521(7553):511–515.

Overstreet C, Klein J, Tillery SH. 2013. Computational modeling of direct neuronal recruitment during intracortical microstimulation in somatosensory cortex. *J Neural Eng*. 10(6): 066016.

Popovych OV, Lysyansky B, Tass PA. 2017. Closed-loop deep brain stimulation by pulsatile delayed feedback with increased gap between pulse phases. *Sci Rep*. 7(1):1033.

Quinkert AW, Schiff ND, Pfaff DW. 2010. Temporal patterning of pulses during deep brain stimulation affects central nervous system arousal. *Behav Brain Res*. 214(2):377–385.

Quiroga RQ, Nadasdy Z, Ben-Shaul Y. 2004. Unsupervised spike detection and sorting with wavelets and superparamagnetic clustering. *Neural Comput*. 16(8):1661–1687.

Rajan AT, Boback JL, Dammann JF, Tenore FV, Wester BA, Otto KJ, Gaunt RA, Bensmaia SJ. 2015. The effects of chronic intracortical microstimulation on neural tissue and fine motor behavior. *J Neural Eng*. 12(6):066018.

Ranck JB Jr. 1975. Which elements are excited in electrical stimulation of mammalian central nervous system: a review. *Brain Res*. 98(3):417–440.

Rebesco JM, Miller LE. 2011. Enhanced detection threshold for in vivo cortical stimulation produced by Hebbian conditioning. *J Neural Eng*. 8(1):016011.

Rebesco JM, Stevenson IH, Koerding K, Solla SA, Miller LE. 2010. Rewiring neural interactions by micro-stimulation. *Front Syst Neurosci*. 4:39.

Renart A, De La Rocha J, Bartho P, Hollender L, Parga N, Reyes A, Harris KD. 2010. The asynchronous state in cortical circuits. *Science*. 327(5965):587–590.

Rieke F. 1999. *Spikes: exploring the neural code*. Cambridge (MA): MIT Press.

Rieke F, Warland D, de Ruyter van Steveninck R, Bialek W. 1997. *Spikes: Exploring the neural code*. Cambridge (MA): MITpress.

Santos FJ, Costa RM, Tecuapetla F. 2011. Stimulation on demand: closing the loop on deep brain stimulation. *Neuron*. 72(2):197–198.

Scarsi F, Tessadori J, Chiappalone M, Pasquale V. 2017. Investigating the impact of electrical stimulation temporal distribution on cortical network responses. *BMC Neurosci*. 18(1):49.

Schmidt E, Bak M, Hambrecht F, Kufta C, O'rourke D, Vallabhanath P. 1996. Feasibility of a visual prosthesis for the blind based on intracortical micro stimulation of the visual cortex. *Brain*. 119(2):507–522.

Shinomoto S, Kim H, Shimokawa T, Matsuno N, Funahashi S, Shima K, Fujita I, Tamura H, Doi T, Kawano K *et al*. 2009. Relating neuronal firing patterns to functional differentiation of cerebral cortex. *PLoS Comput Biol*. 5(7):e1000433.

Skarpaas TL, Morrell MJ. 2009. Intracranial stimulation therapy for epilepsy. *Neurotherapeutics*. 6(2):238–243.

Slomowitz E, Styr B, Vertkin I, Milshtein-Parush H, Nelken I, Slutsky M, Slutsky I. 2015. Interplay between population firing stability and single neuron dynamics in hippocampal networks. *elife*. 4:e04378.

Tabot GA, Dammann JF, Berg JA, Tenore FV, Boback JL, Vogelstein RJ, Bensmaia SJ. 2013. Restoring the sense of touch with a prosthetic hand through a brain interface. *Proc Natl Acad Sci*. 110(45):18279–18284.

Tehovnik E, Tolias A, Sultan F, Slocum W, Logothetis N. 2006. Direct and indirect activation of cortical neurons by electrical microstimulation. *J Neurophysiol*. 96(2):512–521.

Tehovnik EJ, Slocum WM. 2013. Electrical induction of vision. *Neurosci Biobehav Rev*. 37(5):803–818.

Thomson EE, Carra R, Nicolelis MA. 2013. Perceiving invisible light through a somatosensory cortical prosthesis. *Nat Commun*. 4:1482.

Tkačik G, Marre O, Amodei D, Schneidman E, Bialek W, Berry MJ II. 2014. Searching for collective behavior in a large network of sensory neurons. *PLoS Comput Biol*. 10(1): e1003408.

Torab K, Davis T, Warren D, House P, Normann R, Greger B. 2011. Multiple factors may influence the performance of a visual prosthesis based on intracortical microstimulation: nonhuman primate behavioural experimentation. *J Neural Eng*. 8(3):035001.

Vassanelli S, Mahmud M. 2016. Trends and challenges in neuroengineering: toward "intelligent" neuroprostheses through brain-"brain inspired systems" communication. *Front Neurosci*. 10:438.

Vassanelli S, Mahmud M, Girardi S, Maschietto M. 2012. On the way to large-scale and high-resolution brain-chip interfacing. *Cogn Comput*. 4(1):71–81.

Weaver FM, Follett KA, Stern M, Luo P, Harris CL, Hur K, Marks WJ, Rothlind J, Sagher O, Moy C. 2012. Randomized trial of deep brain stimulation for Parkinson disease thirty-six-month outcomes. *Neurology*. 79(1):55–65.

Wyckhuys T, Boon P, Raedt R, Van Nieuwenhuyse B, Vonck K, Wadman W. 2010a. Suppression of hippocampal epileptic seizures in the kainate rat by Poisson distributed stimulation. *Epilepsia*. 51(11):2297–2304.

Wyckhuys T, Raedt R, Vonck K, Wadman W, Boon P. 2010b. Comparison of hippocampal deep brain stimulation with high (130 Hz) and low frequency (5 Hz) on afterdischarges in kindled rats. *Epilepsy Res*. 88(2–3): 239–246.

Zakiewicz IM, Bjaalie JG, Leergaard TB. 2014. Brain-wide map of efferent projections from rat barrel cortex. *Front Neuroinform*. 8:5.